

Marten H. van Kerkwijk · David L. Kaplan

Isolated neutron stars: Magnetic fields, distances, and spectra

Received: date / Accepted: date

Abstract We present timing measurements, astrometry, and high-resolution spectra of a number of nearby, thermally emitting, isolated neutron stars. We use these to infer magnetic field strengths and distances, but also encounter a number of puzzles. We discuss three specific ones in detail: (i) For RX J0720.4–3125 and RX J1308.6+2127, the characteristic ages are in excess of 1 Myr, while their temperatures and kinematic ages indicate that they are much younger; (ii) For RX J1856.5–3754, the brightness temperature for the optical emission is in excess of that measured at X-ray wavelengths for reasonable neutron-star radii; (iii) For RX J0720.4–3125, the spectrum changed from an initially featureless state to one with an absorption feature, yet there was only a relatively small change in T_{eff} . Furthermore, we attempt to see whether the spectra of all seven sourced, in six of which absorption features have now been found, can be understood in the context of strongly magnetised hydrogen atmospheres. We find that the energies of the absorption features can be reproduced, but that the featureless spectra of some sources, especially the Wien-like high-energy tails, remain puzzling.

Keywords Atomic processes and interactions · Stellar Atmospheres · Neutron Stars

PACS 95.30.Dr · 97.10.Ex · 97.60.Jd

M. H. van Kerkwijk
Department of Astronomy & Astrophysics
University of Toronto
60 Saint George Street
Toronto, Ontario M5S 3H8
Canada
Tel.: +1-416-9467288
Fax: +1-416-9467287
E-mail: mhvk@astro.utoronto.ca

D. L. Kaplan
Kavli Institute for Astrophysics and Space Research
Massachusetts Institute of Technology
77 Massachusetts Ave, Room 37-664H
Cambridge, MA 02139
USA
Tel.: +1-617-2537294
Fax: +1-617-2530861
E-mail: dlk@space.mit.edu

1 Introduction

One of the great benefits of the *ROSAT* All-Sky Survey (Voges et al. 1996) is that it has provided an unbiased sample of all classes of nearby neutron stars (limited only by their age and distribution of the local interstellar medium). Particularly interesting is the discovery of the group of seven nearby, thermally emitting, isolated neutron stars (INS; for a review, see Haberl, these proceedings).

The INS form the majority among the nearby neutron stars (typical distances are less than ~ 500 pc; Kaplan et al. 2002b; see also Posselt, Popov, these proceedings), yet are atypical of the neutron-star population represented by radio surveys: while pulsars detected by their thermal emission all have normal periods of less than a second, five out of the seven INS have periods about ten times longer (the remaining two appear to have no pulsations despite intensive searches; Ransom et al. 2002; van Kerkwijk et al. 2004). A number of models — accretors (Wang 1997), middle-aged magnetars (Heyl & Kulkarni 1998; Heyl & Hernquist 1999), long-period pulsars (Kaplan et al. 2002a; Zane et al. 2002) — have been suggested to explain these objects.

A prime reason for studying the INS is the hope of constraining fundamental physics at very high densities: neutron stars are natural laboratories for quantum chromodynamics (Rho 2000). The overall goal is to determine the masses and radii of a number of neutron stars and hence constrain the equation of state (EOS) of ultra-dense matter (Lattimer & Prakash 2000; Lattimer, these proceedings). For the majority of known neutron stars (i.e., radio pulsars), this is complicated by the non-thermal emission that dominates the spectrum, but for the INS this is not the case: the X-ray spectra show thermal emission only. Hence, much effort has been spent trying to derive constraints from the INS (Burwitz et al. 2001, 2003; Drake et al. 2002; Pons et al. 2002). The constraints have not been very meaningful, however, because the data could not be interpreted properly: they just do not fit any current realistic models (Motch et al. 2003; Zane et al. 2004).

To make progress in understanding the thermal emission, we need first to know the basic ingredients: the elemental abundances, the temperature distribution, and the magnetic field strength. Furthermore, to use the thermal emission to infer radii, we need information about the distance. Fortunately, observational clues are now becoming available: broad absorption features at energies of 0.3–0.7 keV have been discovered in the spectra of six of the seven INS (Haberl et al. 2003, 2004b,a; van Kerkwijk et al. 2004; Zane et al. 2005; see Haberl, these proceedings), and, as described below, magnetic field strengths have been inferred from timing solutions and new or improved parallaxes have been measured.

The outline of this contribution is as follows. First, in §2, we present timing solutions for RX J0720.4–3125 and RX J1308.6+2127, and discuss the resulting estimates of the magnetic field strengths and characteristic ages. Next, in §3, we describe new parallax distance measurements for RX J1856.5–3754 and RX J0720.4–3125. For the former, these resolve previous conflicting results, but also raise a puzzle: a rather large radius or high brightness temperature inferred for the optical emission. In §4, we turn to high-resolution X-ray spectra, comparing spectra of RX J0720.4–3125, before and after its spectral change, with those of RX J1308.6+2127. In §5, we attempt to interpret the observations assuming the sources have gaseous atmospheres, focussing on hydrogen, but also briefly discussing the possibility of helium. We summarise and discuss future work in §6.

From here on, we will refer to the INS in the text using abbreviated names: J0420 for RX J0420.0–5022, J0720 for RX J0720.4–3125, J0806 for RX J0806.4–4123, J1308 for RX J1308.6+2127 = RBS 1223, J1605 for RX J1605.3+3249, J1856 for RX J1856.5–3754, J2143 for RX J2143.0+0654 = RBS 1774 = RXS J214303.7+065419.

2 Timing solutions

Until recently, the typical magnetic field strength of the INS was just a guess, with a wide range of possibilities (10^{10} – 10^{15} G) – similar to the wide uncertainty in magnetic field strength implied for the different demographic models of the INS, although based on the long spin periods fields of a few 10^{13} G were considered most likely.

We have improved upon this situation using dedicated timing observations with *Chandra*, which, combined with *Chandra*, *XMM-Newton*, and *ROSAT* archival observations, allowed us to determine phase-coherent timing solutions for J0720 and J1308 stretching back at least 5 years (Kaplan & van Kerkwijk 2005a,b). Using the periods and the period derivatives to place these objects on the classic P - \dot{P} diagram (Fig. 1), one sees that they are intermediate between radio pulsars and magnetars (in line with the idea that they are long-period pulsars whose radio beams do not cross our line of sight; Kaplan et al. 2002a; Zane et al. 2002).

From the solutions, assuming the sources spin down by magnetic dipole radiation, one infers that they have similar magnetic fields: $B = 2.4 \times 10^{13}$ G and 3.4×10^{13} G for

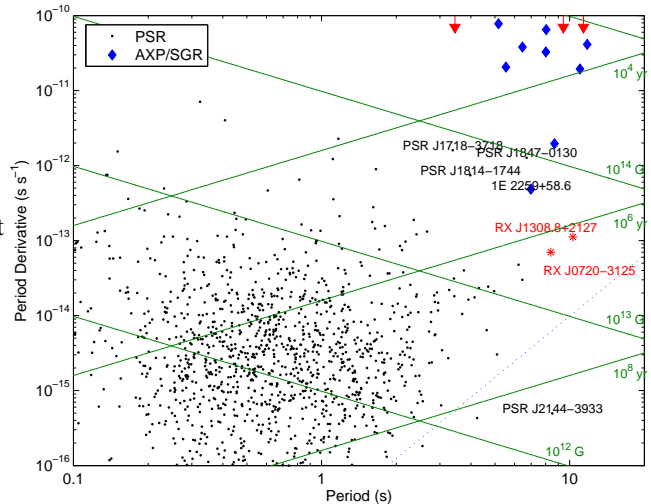


Fig. 1 P - \dot{P} diagram, showing radio pulsars (points) and magnetars (diamonds); selected objects are labeled. Also shown are the five INS with periodicities: RX J0720.4–3125 and RX J1308.6+2127 are shown by the stars, while RX J0420.0–5022, RX J0806.4–4123, and RX J2143.0+0654 are the arrows at the top (since \dot{P} is unknown). The diagonal lines show loci of constant dipole magnetic field and spin-down age, as labeled.

J0720 and J1308, respectively. As will become clear below (§5), this agrees quite well with the magnetic field strengths inferred from the absorption lines.

One also infers characteristic ages: $\tau_c \equiv P/2\dot{P} = 1.9$ Myr for J0720 and 1.5 Myr for J1308. These are puzzling, since they are substantially longer than expected based on cooling: From standard cooling curves (Page et al. 2004), the observed temperatures around 90 eV (10^6 K) correspond to ages of a few 10^5 yr. Even if one takes into account that the black-body temperature likely overestimates the effective temperature – as is clear from the fact that the extrapolation of a black-body fit to the X-ray data underpredicts the optical – one is very hard-pressed to find an age in excess of 10^6 yr; at 1.5 Myr, the effective temperature should be below 20 eV.

For J0720, there is an additional age estimate from kinematics (Motch et al. 2003; Kaplan 2004; also Motch, these proceedings): tracing back its proper motion, the most natural birthplace is the Trumpler 10 association; it would have left about 7×10^5 yr ago. (Note that a possible origin in the Scorpius OB associations about 1.5 Myr ago has also been suggested, but the new parallax and proper motion we derived [partly described in §3 below] make this less likely. Furthermore, for J1856, which is cooler than J0720, the kinematic age of about 4×10^5 yr is not in doubt.)

Of course, the above discrepancy may simply mean that the characteristic age is a poor estimate of the true age. For breaking with $\dot{v} \propto v^n$, where v is the spin frequency and n the so-called braking index (equal to 3 for magnetic dipole radiation), the true age is $t = (1 - P_0/P)^{n-1} (P/(n-1)\dot{P})$. Thus, one can obtain ages $t \ll \tau$ either if the initial spin pe-

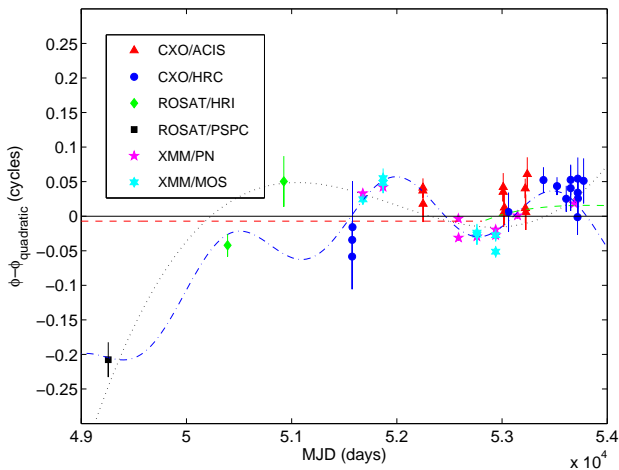


Fig. 2 Phase residuals for timing measurements for RX J0720.4–3125 relative to the best-fit quadratic ($\ddot{\nu} = 0$) model. The data include those from Kaplan & van Kerkwijk (2005a), plus a number of additional points from *Chandra* with LETG/HRC and one additional point from *XMM-Newton* with EPIC-PN (all at MJD > 53500); other EPIC-PN data exist (Haberl, these proceedings) but they are not yet public. The fit has $\chi^2_{\nu} = 11.93$ and the residuals have rms = 0.39 s. We also show alternate fits: the best-fit cubic model ($\ddot{\nu} \neq 0$; dotted, black curve), which has rms = 0.36 s and $\chi^2_{\nu} = 5.12$; the best-fit periodic model (dot-dashed, blue), which has a period of 4.3 yr and rms = 0.23 s and $\chi^2 = 2.35$; and a simple glitch model (dashed, red) with the glitch occurring at MJD 52821, which does not substantially improve the fit over the quadratic model. Note that there appears to be high-frequency residuals that are not fit by any of these models, as can be seen by the disagreement between simultaneous XMM observations with different instruments. Whether these are due to the energy dependence of the pulse profile or some instrumental effect, we cannot say, but it suggests that caution should be taken in interpreting the timing residuals.

riod P_0 is close to the current one (i.e., the neutron star was born spinning slowly, but in no other systems is there evidence for $P_0 > 1$ s), or if n is substantially larger than 3. Lyne (these proceedings) presented evidence for values of n substantially different from 3, although most values were less, implying characteristic ages that are longer than the true age, contrary to what is required here.

As an alternative, we noted that one way of obtaining $P_0 \simeq P$, would be to have the neutron star undergo a phase in which it was accreting, either from a companion (which later disappeared, e.g., in a supernova explosion) or perhaps a fall-back disk such as that discovered around the AXP 4U 0142+61 (Wang et al. 2006). Intriguingly, the equilibrium spin period, $P_{\text{eq}} \approx 5 \text{ s} (B/10^{13} \text{ G})^{6/7} (\dot{M}/\dot{M}_{\text{Edd}})^{-3/7}$, is roughly equal to the current observed periods for a magnetic field of a few 10^{13} G and an accretion rate \dot{M} close to the Eddington rate \dot{M}_{Edd} .

Finally, comparing the timing residuals, we find that for J0720, they are ~ 0.3 s, far larger than the measurement errors, while for J1308, they are consistent with the measurement errors, at ~ 0.01 s. The larger residuals for J0720 have been ascribed to precession (Haberl et al. 2006; also Haberl, these proceedings). To verify this, we tried including differ-

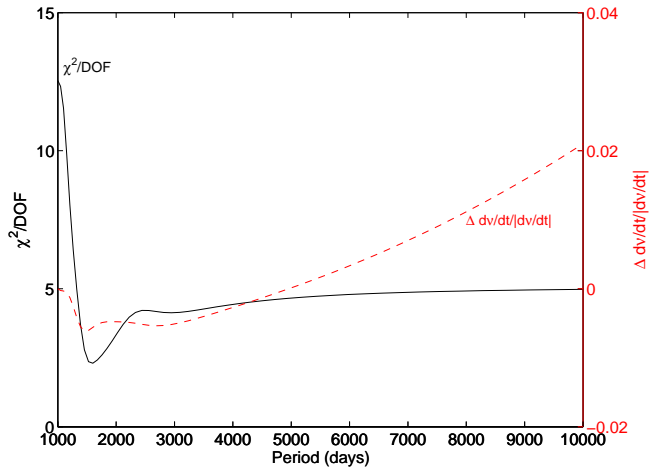


Fig. 3 Improvement in χ^2_{ν} for a timing model for RX J0720.4–3125 that includes a periodic component, as a function of period, fit to the data shown in Fig. 2. The χ^2_{ν} (solid, black curve) has its deepest minimum around 1580 days (4.3 yr); there may be a second minimum near 3000 days (8.2 yr), close to the ~ 7 yr period suggested by Haberl et al. (2006), but with these data it is clearly less significant. Also shown is the fractional change in $\dot{\nu}$ for the different fits (dashed, red curve); it changes by $< 2\%$ for the full range of periods considered here, and thus does not influence the conclusions regarding the magnetic field or characteristic age.

ent terms in our timing model (see Fig. 2), and we indeed find that adding a periodic component improves the fit drastically, with the reduced χ^2 decreasing from $\chi^2_{\nu} = 11.9$ to 2.4. Trying different periods, however, the best period appears to be 4.3 yr (Fig. 3), and not ~ 7 yr as inferred from the spectral changes (at 7 yr, the fit is better than quadratic, but not that much different from a higher-order polynomial). We caution, though, that the timing residuals shown by J0720 are not exceptional: they are in line with trends seen for radio pulsars and similar apparent periodicities can be seen in the residuals of some of the Anomalous X-ray Pulsars (Kaspi, these proceedings).

3 Parallax Measurements

A parallax measurement for the brightest INS, J1856, was first attempted by Walter (2001), using three observations with the Planetary Camera onboard the *Hubble Space Telescope* (*HST*); the resulting parallax implied a distance of ~ 60 pc. The measurement was tricky, however, and a much larger distance of 140 pc was derived from the same observations by Kaplan et al. (2002b); a larger distance, of 117 pc, was also found by Walter & Lattimer (2002), who redid their analysis and included a fourth PC observation.

In order to obtain more accurate distances, we have used the High-Resolution Camera (HRC) of the Advanced Camera for Surveys (ACS) onboard *HST*. This camera is more sensitive than the PC and has a smaller pixel scale, so that undersampling of the point-spread function is much less of

an issue. Furthermore, across the pixels, the sensitivity is more uniform, reducing the variability in the point-spread function with pixel phase; as a result, much more accurate astrometry can be done with ACS/HRC (Anderson & King 2006). We obtained images of J1856 and J0720 in the blue F475W band, visiting each source eight times over two years.

For J1856, our analysis of the HRC data is virtually complete (Kaplan, van Kerkwijk, & Anderson, in preparation). In order to obtain as accurate a parallax as possible, we have taken into account the parallactic motion of the background reference stars, by determining their photometric parallaxes (assuming they are main-sequence stars; for the less distant stars – generally the brighter ones with strong weight – we confirm the photometric parallaxes astrometrically). With that, from the HRC data alone, we determine a parallax $\pi = 6.2 \pm 0.6$ mas, corresponding to a distance $d = 161_{-14}^{+18}$ pc. We are currently trying to improve the measurement further by including the PC data.

For J0720, a first analysis of the HRC data has just been completed. For this source, parallaxes of the background stars are much less important, since it is at low Galactic latitude and most objects are distant. Our preliminary parallax is $\pi = 3.0 \pm 1.0$ mas, corresponding to a distance $d = 330_{-80}^{+170}$ pc.

The factor two ratio in the distances to J1856 and J0720 is consistent with what was expected by Kaplan et al. (2002b) under the zeroth-order assumption that the optical flux for different sources scales as $f_v \propto T(R/d)^2$, that the radii R are similar, and that the temperature T in the region of the atmosphere emitting the optical emission scales with the temperature determined from fits to the X-ray spectrum. The distances also compare well with the distances of 135 ± 25 and 255 ± 25 pc inferred from the run of H I column density with distance (Posselt, these proceedings).

With our distances, we can estimate the radii for the two sources. We start by simply using the black-body fit to the X-ray spectra. For J1856, one finds $kT = 63$ eV and $R_\infty/d = 0.0364$ km pc $^{-1}$, which, with our new distance, implies a radiation radius $R_\infty \simeq 6.5$ km. This is smaller than a typical radius of a neutron star, but this is not unexpected, for two reasons. First, for the most likely atmospheric compositions, the opacity decreases with increasing frequency. As a result, at X-ray energies one sees relatively hot layers and a fit to the X-ray spectrum will thus overestimate the effective temperature and underestimate the radius (Pavlov et al. 1996). Second, the temperature distribution likely is not uniform, in which case the area inferred from the X-ray emission would simply correspond to that of the hotter parts.

In the above picture, one expects the optical emission to be in excess of the extrapolation from the black-body fit, since it arises from a cooler layer and from a larger area. And indeed, the spectral energy distribution, shown in Fig. 4, shows an excess. It poses a possible problem, however, since the optical excess is a factor 7, which implies a radiation radius of $R_{\infty, \text{opt}} = 17(T_X/T_{\text{opt}})^2$ km (where T_{opt} and T_X are suitable averages of the temperatures of the optical and X-ray emitting regions, respectively). Given that one expects

$T_{\text{opt}} < T_X$, the optical emission thus seems to imply that the radiation radius is quite a bit larger than 17 km. Yet, for most reasonable equations of state, a typical neutron star will have a smaller radiation radius (e.g., Lattimer & Prakash 2001).

Of course, the above discrepancy may simply reflect our lack of understanding of neutron star atmospheres in strong magnetic fields: the temperature of the optical emission region may be larger than expected. In order to see what would be required, one can reverse the process: assume that the neutron star has a ‘standard’ mass and radius, and calculate the brightness temperature at each energy assuming that the emission originates from the whole surface. In Fig. 5, we show the result for $R_\infty = 14.7$ km (which is the value one obtains for $M = 1.35 M_\odot$ and $R = 12$ km). We see that this confirms the above reasoning: in order to produce the optical emission, the temperature in the emission region has to exceed 70 eV, i.e., be higher than that in the X-ray emitting region.

For J0720, a fit to the X-ray spectrum from 2000 (i.e., before the appearance of an absorption line) gives $kT = 85.7$ eV and $R_\infty/d = 0.0170$ km pc $^{-1}$. Taking the distance at face value, the implied radiation radius is 5.7 km, a little smaller than that of J1856, but easily consistent within the 30% uncertainty due to the parallax measurement error. Since the optical excess is similar, the radiation radius for the optical emission is again large. In this case, however, the optical emission does not follow a Rayleigh-Jeans tail (Kaplan et al. 2003; Motch et al. 2003; Fig. 4), and hence it is not clear that the emission is from the surface. This can also be seen from the brightness temperatures (Fig. 5), which is not constant in the optical/ultraviolet range.

A further puzzle raised in comparing the sources, is that despite the fact that the X-ray emission areas are rather similar, the pulsation properties are very different: J0720 shows clear pulsations, with a pulsed fraction of 11% (Haberl et al. 1997), while J1856 shows no pulsations, to a limit of $\sim 1\%$ (Ransom et al. 2002; Burwitz et al. 2003). This may reflect differences in geometry; for isotropic emission from two opposite magnetic poles, there is a fair range in parameters for which no pulsations would be observed (e.g., Beloborodov 2002). Of course, the presence of the pulsations constitutes a warning about the brightness temperatures shown in Fig. 5: if the X-ray emission does not arise from the whole surface, the true temperatures will be higher than those shown.

4 LETG spectra

The study of the X-ray spectra of the INS has made great strides with the advent of *Chandra* and *XMM-Newton*. Both the CCD instruments, in particular EPIC-PN, and the grating spectrometers LETG and RGS have been used extensively. Here, we focus on the grating instruments (for the exciting results from EPIC-PN, see Haberl, these proceedings). We will only discuss results from LETG, since that instrument covers the full range of energies at which INS emit and since

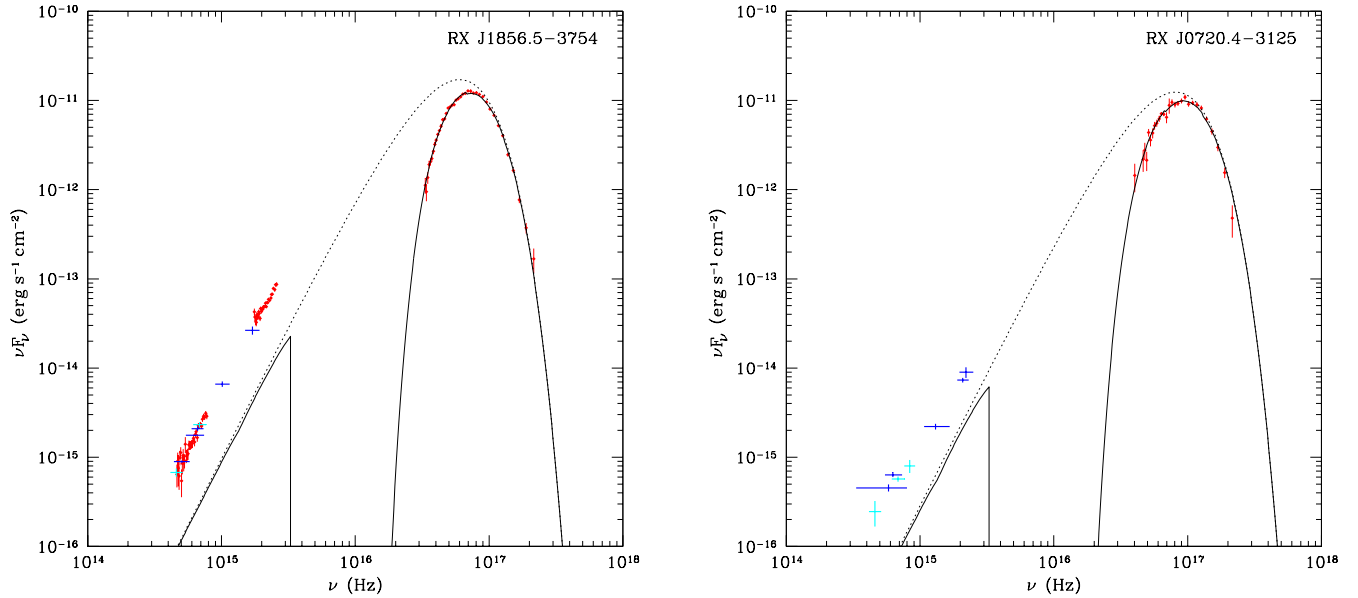


Fig. 4 Spectral energy distributions for RX J1856.5–3754 (left) and RX J0720.4–3125 (right; with the X-ray spectrum from before the appearance of an absorption feature). For both, the X-ray points are from LETG spectra, the dark blue points from *HST*, and the cyan points from ground-based observations. The optical and ultraviolet spectra for RX J1856.5–3754 are from VLT and *HST*, respectively. The black, drawn curves represent the best-fit black-body models to the X-ray data; the dotted curves are the same model without interstellar extinction.

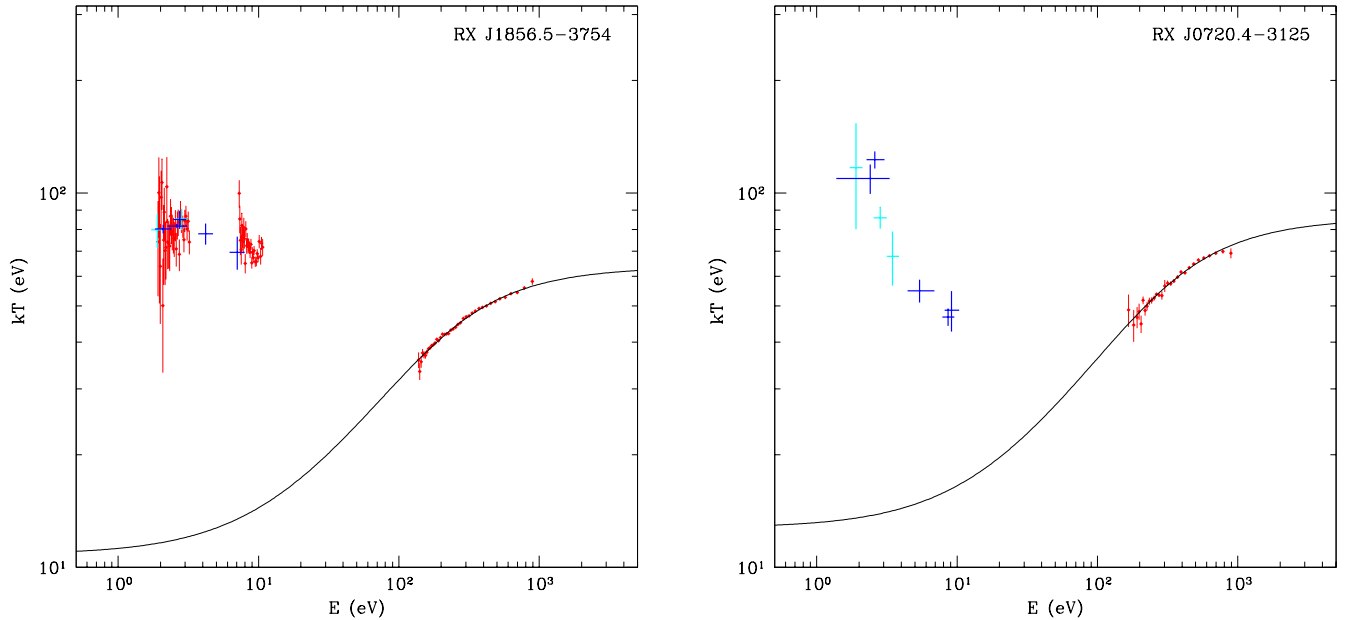


Fig. 5 Brightness temperatures for RX J1856.5–3754 (left) and RX J0720.4–3125 (right), assuming our parallax measurements are correct and that the emission arises from a neutron star with radiation radius $R_\infty = 14.7$ km (which is the value one obtains for $M = 1.35 M_\odot$ and $R = 12$ km). The symbols and colours are as in Fig. 4 (the model curves are not at a constant temperature since the best-fit radiation radius is not equal to 14.7 km). One sees that the optical emission requires temperatures at least equal to those required for the X-ray emission. Note, however, that for RX J0720.4–3125 it is not clear the emission is thermal.

the calibration of the RGS at longer wavelengths has been rather problematic.¹

So far, three sources have been observed with LETG. By far the best spectrum is of J1856, taken using 500 ks of

director’s discretionary time. Unfortunately, and puzzlingly, the spectrum appears completely featureless, and is well described by a black-body model (Burwitz et al. 2001, 2003; Drake et al. 2002; Braje & Romani 2002). The second brightest source, J0720 has been studied extensively as well. A first spectrum was taken in 2000 (Kaplan et al. 2003), when

¹ The problems appear to be largely solved with the 2006 June 30 release of the Scientific Analysis Software.

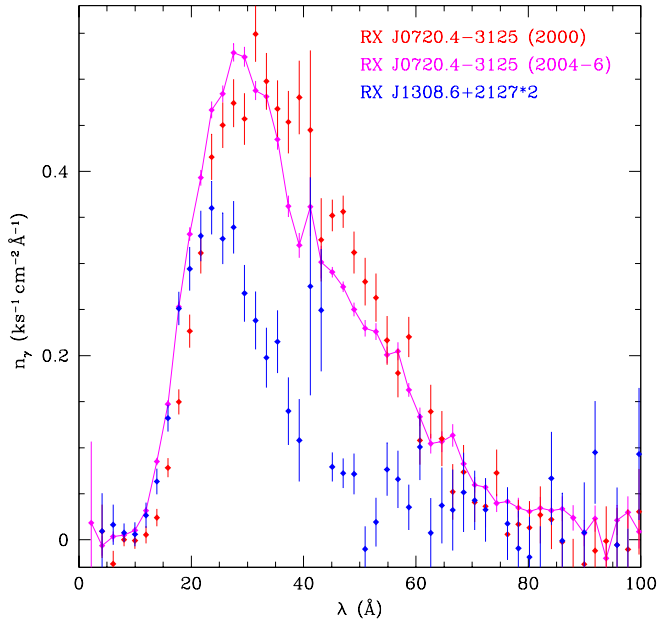


Fig. 6 Spectra of RX J0720.4–3125 and J1308.6+2127 taken with LETG. The magenta points connected with the line are the average of spectra of RX J0720.4–3125 taken after 2004 (about 300 ks). Compared to the earlier spectrum (red points), the spectrum is harder and has developed an absorption feature. On the other hand, compared to RX J1308.6+2127 (blue points, multiplied by two in order to match at the short-wavelength side), the feature is rather weak, even though the inferred temperature is similar (as is also clear from the good match at short wavelengths), and so is the magnetic field inferred from timing.

the spectrum was featureless, and a second in 2004 (Vink et al. 2004), to confirm the change in spectrum discovered with RGS by de Vries et al. (2004). During 2005, the source was regularly monitored by us, for 300 ks total, in order to look for further spectral changes and to see if more than one spectral feature was present. Finally, a 100 ks observation was made of J1308 in guaranteed time by the MPA group.

In Fig. 6, we show the LETG spectra of J0720 and J1308. For the former, we show separately the ‘before’ spectrum (from 2000, before the appearance of an absorption feature) and the ‘after’ spectrum (the average of all spectra taken after the change; within our statistics, the individual spectra do not differ).

The comparison of the three spectra raises a number of questions. First, for J0720, how can a relatively small change in temperature (from ~ 80 to 90 eV) cause the appearance of a pronounced absorption feature? Second, independent of the state of J0720, why is the absorption feature much less strong than that in J1308, despite the fact that their temperatures and magnetic field strengths (from timing, §2) are rather similar?

Considering first the change in J0720, the simplest possibility would be that the increase in temperature corresponds to a relatively large change in the ionisation and/or dissociation balance. If so, this might give a clue to the corresponding energies of the matter in the atmosphere. The alternative would be that the region that heated up (or appeared in view)

has either a different composition or a greatly different magnetic field strength compared to the regions that dominated the spectrum before the change. Neither possibility seems particularly appealing.

Whatever the physical reason for the appearance of the absorption feature, another more basic question is whether the change corresponds to a global change in the properties, or whether, instead, only a fraction of the surface changed or if one’s viewpoint changed. A global change might occur if, e.g., heat was deposited deep inside the neutron star. In contrast, a change in a limited area would be expected if heat were deposited near the surface (with the affected area perhaps increasing in size with time), or if the source were precessing and different regions came into view (de Vries et al. 2004; Haberl et al. 2006; Haberl, Zane, these proceedings).

Of course, if only part of the area that we see changed, then the average ‘after’ spectrum we currently observe contains a contribution from the unchanged parts of the surface, i.e., from the cooler, featureless ‘before’ spectrum. Hence, the spectrum from the changed part should be hotter and should have a stronger line than one would infer from the average. We can set an upper limit to the contribution from the ‘before’ spectrum by requiring that it does not exceed the ‘after’ spectrum at any wavelength. From Fig. 6, one sees that the limit is about 70%, set by the 35–40 Å region.

The above could solve the second question: it might well be that after the change, the parts of the surface of J0720 that show an absorption feature in their spectrum, have a line as strong as that observed in J1308. It only appears weaker in the ‘after’ spectrum because it is diluted by the featureless emission from the unchanged parts of the surface. So, just a single question may be left: how can a neutron-star atmosphere, with presumably the same magnetic field strength and the same composition, and with only a modest, $\Delta T/T < 0.2$ temperature increase, emit such different spectra?

5 Strongly magnetised atmospheres

In interpreting the spectra, a major uncertainty is the composition. For a single source, this may be difficult to determine uniquely, but one can hope to make progress by treating the INS as an ensemble: ideally, it should be possible to understand the features (or lack thereof) in all INS with a single composition, appealing only to differences in temperature and magnetic field strength (constrained by observations where possible), which might lead to different ionisation states being dominant, and possibly the formation of molecules or even a condensate. Here, we discuss only the possibilities of hydrogen or helium atmospheres. For completeness, we note that gaseous atmospheres composed of heavier elements appear to be excluded by the lack of large numbers of features. Condensates from heavier elements are also being considered seriously (Pons, Ho, these proceedings), and detailed theoretical calculations are being carried out to determine at what magnetic field strength condensates can form (Medin & Lai 2006; Lai, these proceedings).

5.1 Hydrogen

The presence of a hydrogen atmosphere has often been considered by default, since if any hydrogen is present, gravitational settling will ensure it floats to the surface. Typically, it has been assumed the hydrogen is fully ionised, and spectral features have been interpreted as proton cyclotron lines. In strong magnetic fields, however, the binding energies of atoms increase (for a review, Lai 2001; Potekhin, these proceedings; see also Fig. 7), and for temperatures and fields appropriate for INS, a fraction of up to 10% of neutral hydrogen will be present (Potekhin et al. 1999). From initial model-atmosphere calculations that take the presence of neutral hydrogen into account (Ho et al. 2003, see their Fig. 3), it is clear that, e.g., at 10^6 K and 10^{13} G, the lines from neutral hydrogen have larger equivalent width than the proton cyclotron line (they are less deep but much wider, due to the so-called motional Stark effect; Pavlov & Meszaros 1993; Potekhin & Pavlov 1997); at lower temperatures or stronger magnetic fields, the fraction of neutral hydrogen increases and hence the difference should be even larger. In general, it is worth stressing that the features are very strong: they may not appear so on the logarithmic scale typically used, but they have depths often exceeding 50%, similar to what is observed for J1308.

Below, we first discuss whether the energies of the main features observed in the INS can be reproduced by a strongly magnetised atmosphere, and then turn to two possible problems: harmonically spaced lines found recently, and the featureless, black-body like spectra shown by some INS. We do not include the optical excess among these problems, since currently it is not clear any model makes reliable predictions for the optical emission: at a few 10^{13} G, the plasma frequency exceeds the frequencies of optical photons, and the models do not take into account the resulting significant deviations of the refractive index from unity (van Adelsberg & Lai 2006; see Kowalski & Saumon 2004 for a discussion of possible effects in the context of cool white-dwarf atmospheres composed of helium).

5.1.1 Line energies

In Fig. 7, we show the energies for features that might be produced in a hydrogen atmosphere: the electron and proton cyclotron lines, and the bound-bound and bound-free transitions of neutral hydrogen (relative to the ground state). Also shown are the approximate energies of the main features that have been detected in the various INS (corrected for an assumed gravitational redshift of 0.3)

In the figure, thick vertical lines indicate the two magnetic field strengths inferred from timing (§2). From those, it follows that if J0720 and J1308 have hydrogen atmospheres, the features are most likely due to the transition from the ground state to the first excited tightly bound state of neutral hydrogen, perhaps in combination with the proton cyclotron line. As argued in §4 above, the line in J0720 might be weaker than that in J1308 because the emission from part

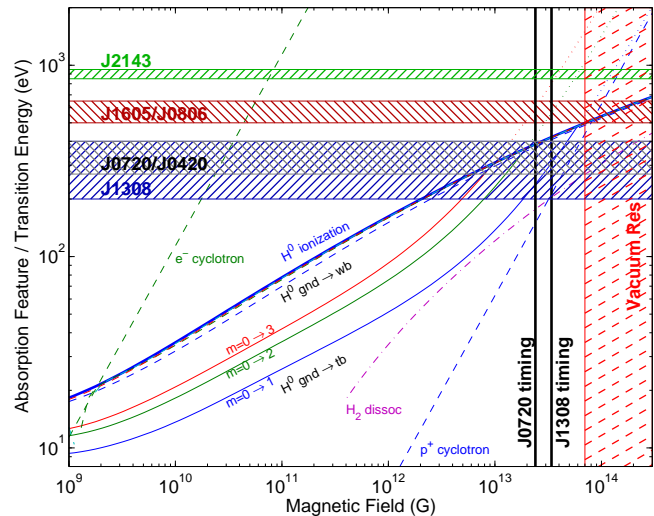


Fig. 7 Energy versus magnetic field for electron and proton cyclotron, ground state to tightly bound (tb) or weakly bound (wb) states in neutral hydrogen, hydrogen ionisation, and molecular H_2 dissociation (Ho et al. 2003; Lai 2001; Potekhin 1998). For fields above $\sim 10^{14}$ G (hatched region to the right), features may be washed out due to the effects of vacuum resonance mode conversion (Lai & Ho 2003). The hatched bands show the energies of the main absorption features (corrected for gravitational redshift) for the INS, and the two vertical lines indicate the dipole field strengths determined by timing. The sources are labeled with short-hand notation as in the text (see end of §1). References for the energies are: J0420, Haberl et al. (2004a); J0720, Haberl et al. (2004b); J0806, Haberl et al. (2004a); J1308, Haberl et al. (2003); J1605, van Kerkwijk et al. (2004); J2143, Zane et al. (2005).

of its surface is featureless (which in itself is problematic; we return to this below). Alternatively, the line in J0720 might be weaker because it is to the second excited tightly bound state (van Kerkwijk et al. 2004).

If the above is correct, the feature in J0420 likely has the same origin and thus its field should also be a few 10^{13} G. The features in J1605 and J0806 could result from the same transitions or from the ionisation edge, but in either case the implied magnetic field strength is higher, close to 10^{14} G. For J1605, van Kerkwijk et al. (2004) noted that the line was substantially weaker than that of J1308, and they suggested this might be due to the effect of vacuum resonance mode conversion, which for fields in excess of $\sim 7 \times 10^{13}$ G tends to weaken features (see Ho & Lai 2003; also Lai, these proceedings). Finally, for J2143, the line energy of 0.7 keV is substantially higher than what is observed for all other sources, and for any transition in neutral hydrogen, the upper state is auto-ionising: it is at an energy level that is higher than the continuum from the ground state. It is thus not clear whether the line could be due to neutral hydrogen. Instead, it might be due to the proton cyclotron line in a field of just over 10^{14} G. For these field strengths, the feature should be strongly weakened by vacuum resonance mode conversion (but not necessarily disappear; e.g., Ho & Lai 2004; van Adelsberg & Lai 2006); qualitatively, this is consistent with the rather modest observed strength Zane et al. (2005).

5.1.2 Possible problem 1: Harmonically spaced lines

At the conference, evidence for harmonically spaced absorption lines was presented for three INS. For J1605, Haberl (these proceedings) found that apart from the line at 0.40 keV discovered by van Kerkwijk et al. (2004), the EPIC-PN data show a significant feature at 0.78 keV, i.e., at an energy that is in a 1:2 ratio with that of the stronger line. Furthermore, a third feature at 0.59 keV could be present, consistent with energies in a 2:3:4 ratio. For J1308, Schwöpe et al. (these proceedings) presented evidence that the single strong feature originally found at 0.3 keV or less by Haberl et al. (2003), could be composed of two features, at 0.23 and 0.46 keV, i.e., again harmonically spaced. Finally, for J0806, the single feature at 0.43 keV found by Haberl et al. (2004a) may again be better described by two features at 0.30 and 0.60 keV (Haberl, these proceedings).

It would appear tempting to interpret these features as cyclotron lines, since those naturally have harmonic energy ratios. It is difficult, however, to see how this could be possible for proton cyclotron lines, since the harmonics are expected to be exceedingly weak: the oscillator strength for the harmonic would be a factor $E/m_p c^2$ weaker than that for the fundamental.

Instead, as mentioned in a discussion with George Pavlov, Joachim Trümper, and Frank Haberl at the meeting, a different solution may be suggested by the behaviour of the transitions of neutral hydrogen. As can be seen in Fig. 7, for any transition, above a certain magnetic field strength, the transition energy starts to become proportional to the proton cyclotron energy. As a result, at sufficiently strong magnetic field, the transitions become harmonically related. A possible problem, however, is that in this situation, the upper level of the transition is an auto-ionising state, i.e., it has an energy in excess of the continuum energy relative to the ground state. It will still lead to some additional opacity, but at present it is not clear whether this is sufficient. Fortunately, there is one prediction: for J1605, it would not be possible to explain the spectrum if there are really three features in a 2:3:4 ratio, without a strong corresponding ‘1’; thus, the prediction is that upon further analysis, the 0.59 keV feature will disappear.

Finally, we note in this context that it will be worth checking carefully that for J2143, the 0.7 keV feature observed is in fact not a ‘harmonic.’ From the present fits by Zane et al. (2005), a rather high N_H is inferred, and this could perhaps be an artefact of a strong absorption feature at ~ 0.3 keV? (From initial attempts, this appears unlikely; Cropper, 2006, pers. comm.)

5.1.3 Possible problem 2: Featureless black-body spectra

Perhaps the most severe problem with the idea that the INS have pure hydrogen atmospheres is that the spectra of J1856 and J0720 (before the change) are featureless and well represented by black-body emission. For J1856, perhaps no features are expected, since its magnetic field strength, as in-

ferred from the bow-shock shaped $H\alpha$ nebula around the source (van Kerkwijk & Kulkarni 2001; Kaplan et al. 2002b), is below 10^{13} G, in which case all features may be below the observed band (Fig. 7), but for J0720 this explanation is not possible. Furthermore, for a mostly ionised atmosphere, the spectrum is expected to have a hard tail, unlike the observed exponential, Wien-like shape, since the free-free opacity decreases with increasing energy.

There are several possible solutions. First, there could be a reason for the opacity to be much greyer than currently estimated, so that the emission at all wavelengths originates from layers at similar depths and thus with similar temperature. The extreme version of this, discussed in detail by Pons and Ho (these proceedings), is that the two sources have a condensed surface (with possibly only a thin hydrogen layer on top). A less extreme version might be that the atmosphere does not contain just ionised and neutral hydrogen, but also molecules, which might have so many transitions that the opacity becomes effectively grey. Hydrogen molecules do indeed have a higher binding energy than hydrogen atoms, but the dissociation energy is only around 0.2 keV for a few 10^{13} G (Lai 2001; see Fig. 7). With temperatures only a factor two smaller, the abundance should be very small (as indeed found by, e.g., Potekhin et al. 1999; see their Fig. 7). Nevertheless, it may be worthwhile verifying this, making sure that the abundance and the resulting opacity are indeed negligible.

A possible alternative way to produce spectra resembling black bodies is by making the temperature profile in the atmosphere shallower, closer to isothermal. While this certainly appears ad hoc and likely would require significant fine-tuning, there is evidence for active magnetospheres: for J1856, the $H\alpha$ nebula provides evidence of a pulsar wind, and for J0720, the optical emission appears to be partly non-thermal. If there is an active magnetosphere, some particles might hit the atmosphere, leading to additional heating; at the right locations, this could lead to rather different emergent spectra (e.g., Gänsicke et al. 2002).

At present, none of the above explanations seem satisfactory. Also, none provide an easy explanation for why some sources have featureless spectra while others have not (or why it would change). Perhaps the first parameter to consider would be the overall temperature, since J1856 is cool and the appearance of the absorption feature in J0720 was accompanied by a temperature increase. The increase was only small ($\Delta T/T < 0.2$), however, and furthermore, an absorption feature does appear to be present in the coolest INS, J0420 ($kT \simeq 45$ eV, Haberl et al. 2004a).

5.2 Helium

Above, we stated that if any hydrogen were present, it would float to the top. Recently, it has been questioned, however, whether an outer hydrogen envelope can survive (Chang & Bildsten 2004; Chang et al. 2004). The reason this is not certain is that some hydrogen will diffuse down and reach underlying

Carbon or Oxygen layers, where, if the temperature is right, it will be burned. Indeed, Chang & Bildsten (2004) find that all of the hydrogen can be burned in the first 10^5 yr of a neutron star's life, in which case an atmosphere composed of helium might be left (unless hydrogen is replenished, as could happen due to spallation by relativistic particles from the magnetosphere, or very low levels of accretion).

Partly inspired by this possibility, Pavlov & Bezchastnov (2005) calculated properties of singly-ionised helium in strong magnetic fields. For a few 10^{13} G, the transition energies are again in the range that features are observed in the INS, and hence it seems worthwhile to try to do a similar analysis as done above for hydrogen. From a very rough first attempt at producing model atmospheres (done by Kaya Mori and Wynn Ho), including neutral helium, it seems that, like for hydrogen, the features will be very strong. Typically, however, more than one very strong feature should be present, which appears to be in conflict with what is observed. The picture is currently incomplete, however, since molecules have not yet been considered, while for helium the binding energy of, e.g., He_2^+ is sufficiently high that it may well be present (a detailed calculation is tricky, since one has to have a decent estimate of the number of possible rotational and vibrational states).

6 Discussion and future prospects

Of the four main parameters mentioned in the introduction that determine the properties of the thermal emission from INS, we now appear to have reasonable handles on three: the shapes of the X-ray spectra indicate temperatures around 10^6 K, period derivatives imply magnetic field strengths of a few 10^{13} G, and parallax measurements show that a fair fraction of the surface is emitting X-ray radiation.

The main unknown appears to be the composition. We found that the energies of the observed absorption features can be matched fairly easily for hydrogen atmospheres. However, reproducing the smooth, featureless spectra of some INS, and the Wien-like high-energy side of the X-ray spectra in general, appears problematic, nor is it clear how the spectrum of J0720 could change from featureless to one that has an absorption line.

Fortunately, it should soon become clear whether these issues are real problems or not, since great progress is being made in constructing more reliable strongly magnetised hydrogen model atmospheres (Lai, Potekhin, these proceedings). From §5, it seems particularly important to include in full detail transitions to the auto-ionising levels, verify that all sources of opacity, including from (traces of) molecules are included, and check the influence, in particular on the temperature profile, of high-density effects and vacuum resonance mode conversion. At the same time, it would seem worthwhile to consider atmospheres of other elements; for the INS, He might be most relevant, but it would be good to check heavier elements as well, since these may cause the

absorption features seen in 1E 1207.4–5209 (Hailey & Mori 2002).

From the observational side, the easiest route to further progress would appear to be timing. With further estimates of the magnetic fields, one can test the predictions based on hydrogen atmospheres, that J0420 has a field about as strong as that of J0720 and J1308, J0806 a stronger one, approaching 10^{14} G, and J2143 the strongest, in excess of 10^{14} G.

For the X-ray spectra, further monitoring is useful, but perhaps the largest advance will come from the unified analysis of all sources, which allows one to exclude instrumental effects. This is already well underway for the EPIC-PN data (Haberl, these proceedings), and similar studies of the LETG and RGS data should prove fruitful. As present, first steps are being taken in detailed modelling of the phase-resolved spectra (Haberl, Zane, these proceedings), and this should help obtain stronger constraints on the thermal distribution over the surface.

Finally, in the optical-ultraviolet regime, it would be good to complete the census of the sources, and obtain at least rough spectral energy distributions, to determine whether the emission is thermal, or whether there are non-thermal components. For sources that are sufficiently bright, proper motion measurements can help determine true ages and parallax measurements can help determine distances.

Acknowledgements It is a pleasure to thank Kaya Mori, Wynn Ho, George Pavlov, and Dong Lai for enlightening discussions about the physics of strongly magnetised, dense atmospheres, and Jay Anderson for his continuing patience and collaboration in trying to extract the best possible astrometry from *HST* images. We acknowledge financial support through a guest observer grant from NASA, as well as through individual grants from NSERC (MHvK) and a Pappalardo fellowship (DLK).

References

- Anderson, J. & King, I. 2006, Multi-filter PSFs and Distortion Corrections for the HRC, ISR 04-15, Space Telescope Science Institute
- Beloborodov, A. M. 2002, *ApJ*, 566, L85
- Braje, T. M. & Romani, R. W. 2002, *ApJ*, 580, 1043
- Burwitz, V., Haberl, F., Neuhäuser, R., Predehl, P., Trümper, J., & Zavlin, V. E. 2003, *A&A*, 399, 1109
- Burwitz, V., Zavlin, V. E., Neuhäuser, R., Predehl, P., Trümper, J., & Brinkman, A. C. 2001, *A&A*, 379, L35
- Chang, P., Arras, P., & Bildsten, L. 2004, *ApJ*, 616, L147
- Chang, P. & Bildsten, L. 2004, *ApJ*, 605, 830
- de Vries, C. P., Vink, J., Méndez, M., & Verbunt, F. 2004, *A&A*, 415, L31
- Drake, J. J. et al. 2002, *ApJ*, 572, 996
- Gänsicke, B. T., Braje, T. M., & Romani, R. W. 2002, *A&A*, 386, 1001
- Haberl, F., Motch, C., Buckley, D. A. H., Zickgraf, F.-J., & Pietsch, W. 1997, *A&A*, 326, 662
- Haberl, F., Motch, C., Zavlin, V. E., Reinsch, K., Gänsicke, B. T., Cropper, M., Schwöpe, A. D., Turolla, R., & Zane, S. 2004a, *A&A*, 424, 635
- Haberl, F., Schwöpe, A. D., Hambaryan, V., Hasinger, G., & Motch, C. 2003, *A&A*, 403, L19
- Haberl, F., Turolla, R., de Vries, C. P., Zane, S., Vink, J., Méndez, M., & Verbunt, F. 2006, *A&A*, 451, L17
- Haberl, F., Zavlin, V. E., Trümper, J., & Burwitz, V. 2004b, *A&A*, 419, 1077

- Hailey, C. J. & Mori, K. 2002, *ApJ*, 578, L133
- Heyl, J. S. & Hernquist, L. 1999, *Phys. Rev. D*, 59, 45005
- Heyl, J. S. & Kulkarni, S. R. 1998, *ApJ*, 506, L61
- Ho, W. C. G. & Lai, D. 2003, *MNRAS*, 338, 233
- , 2004, *ApJ*, 607, 420
- Ho, W. C. G., Lai, D., Potekhin, A. Y., & Chabrier, G. 2003, *ApJ*, 599, 1293
- Kaplan, D. L. 2004, PhD thesis, California Institute of Technology
- Kaplan, D. L., Kulkarni, S. R., van Kerkwijk, M. H., & Marshall, H. L. 2002a, *ApJ*, 570, L79
- Kaplan, D. L. & van Kerkwijk, M. H. 2005a, *ApJ*, 628, L45
- , 2005b, *ApJ*, 635, L65
- Kaplan, D. L., van Kerkwijk, M. H., & Anderson, J. 2002b, *ApJ*, 571, 447
- Kaplan, D. L., van Kerkwijk, M. H., Marshall, H. L., Jacoby, B. A., Kulkarni, S. R., & Frail, D. A. 2003, *ApJ*, 590, 1008
- Kowalski, P. M. & Saumon, D. 2004, *ApJ*, 607, 970
- Lai, D. 2001, *Reviews of Modern Physics*, 73, 629
- Lai, D. & Ho, W. C. G. 2003, *ApJ*, 588, 962
- Lattimer, J. M. & Prakash, M. 2000, *Phys. Rep.*, 333, 121
- , 2001, *ApJ*, 550, 426
- Medin, Z. & Lai, D. 2006, *astro-ph/0607166*
- Motch, C., Zavlin, V. E., & Haberl, F. 2003, *A&A*, 408, 323
- Page, D., Lattimer, J. M., Prakash, M., & Steiner, A. W. 2004, *ApJS*, 155, 623
- Pavlov, G. G. & Bezchastnov, V. G. 2005, *ApJ*, 635, L61
- Pavlov, G. G. & Meszaros, P. 1993, *ApJ*, 416, 752
- Pavlov, G. G., Zavlin, V. E., Truemper, J., & Neuhaeuser, R. 1996, *ApJ*, 472, L33
- Pons, J. A., Walter, F. M., Lattimer, J. M., Prakash, M., Neuhaeuser, R., & An, P. 2002, *ApJ*, 564, 981
- Potekhin, A. Y. 1998, *Journal of Physics B Atomic Molecular Physics*, 31, 49
- Potekhin, A. Y., Chabrier, G., & Shibanov, Y. A. 1999, *Phys. Rev. E*, 60, 2193
- Potekhin, A. Y. & Pavlov, G. G. 1997, *ApJ*, 483, 414
- Ransom, S. M., Gaensler, B. M., & Slane, P. O. 2002, *ApJ*, 570, L75
- Rho, M. 2000, *nucl-th/0007073*
- van Adelsberg, M. & Lai, D. 2006, *astro-ph/0607168*
- van Kerkwijk, M. H., Kaplan, D. L., Durant, M., Kulkarni, S. R., & Paerels, F. 2004, *ApJ*, 608, 432
- van Kerkwijk, M. H. & Kulkarni, S. R. 2001, *A&A*, 380, 221
- Vink, J., de Vries, C. P., Méndez, M., & Verbunt, F. 2004, *ApJ*, 609, L75
- Voges, W. et al. 1996, *IAU Circ.*, 6420, 2
- Walter, F. M. 2001, *ApJ*, 549, 433
- Walter, F. M. & Lattimer, J. M. 2002, *ApJ*, 576, L145
- Wang, J. C. L. 1997, *ApJ*, 486, L119
- Wang, Z., Chakrabarty, D., & Kaplan, D. L. 2006, *Nature*, 440, 772
- Zane, S., Cropper, M., Turolla, R., Zampieri, L., Chierigato, M., Drake, J. J., & Treves, A. 2005, *ApJ*, 627, 397
- Zane, S., Haberl, F., Cropper, M., Zavlin, V. E., Lumb, D., Sembay, S., & Motch, C. 2002, *MNRAS*, 334, 345
- Zane, S., Turolla, R., & Drake, J. J. 2004, *Advances in Space Research*, 33, 531